



The 8th Trondheim Conference on CO<sub>2</sub> Capture, Transport and Storage

## Corrosion evaluation of MEA solutions by SEM-EDS, ICP-MS and XRD

Georgios Fytianos<sup>a</sup>, Seniz Ucar<sup>a</sup>, Andreas Grimstvedt<sup>b</sup>, Hallvard F. Svendsen<sup>a</sup>, Hanna Knuutila<sup>a\*</sup>

<sup>a</sup>Norwegian University of Science and Technology, 7491 Trondheim, Norway

<sup>b</sup>SINTEF Materials and Chemistry, 7465 Trondheim, Norway

---

### Abstract

The target of this work is to evaluate three analytical techniques, ICP-MS, SEM-EDS and XRD, which can be applied in corrosion monitoring of ethanolamine based post-combustion CO<sub>2</sub> capture plants. The work is based on analyses of the solvent and 316 SS cylinders used in thermal degradation experiments. ICP-MS is used for the determination of total Fe, Cr and Ni of the solutions as an indication of corrosivity. Additionally, the cylinder surface was examined with SEM-EDS and XRD was used for the identification of corrosion products. Finally, a discussion is given on the various techniques, their limitations and advantages.

©2015 The Authors. Published by Elsevier Ltd.

Peer-review under responsibility of the Programme Chair of The 8th Trondheim Conference on Capture, Transport and Storage.

*Keywords:* corrosion; MEA degradation; SEM; ICP-MS

---

### 1. Introduction

Corrosion is considered to be one of the most severe operational problems in CO<sub>2</sub> absorption processes and experience shows that amine degradation products often aggravate corrosion. Corrosion has always been an issue in natural gas sweetening using amines. Some of the main forms of corrosion are general corrosion, erosion corrosion, stress corrosion cracking, pitting, crevice and galvanic corrosion [1]. During the last decades a lot of research is

---

\* Corresponding author. Tel.: +47 73594119; fax: + 47 735 94080.

*E-mail address:* [hanna.knuutila@ntnu.no](mailto:hanna.knuutila@ntnu.no)

being done in order to improve the knowledge of corrosion processes in amine units [2]. The corrosion rate depends on the materials used in the CO<sub>2</sub> capture plant. Stainless steel is more resistant to corrosion than carbon steel and most of the important materials of pilot plants are now constructed from stainless steel. Degradation of amines can be oxidative or thermal and some of the degradation products are corrosive agents and inevitably cause equipment corrosion in the absorption plant which leads to additional costs.

When studying corrosion it is of great importance to examine the corrosion rate, the kinetics of corrosion, the products that are formed on the surface, the corrosion type and a possible link between degradation products and corrosion. The weight loss technique with metal coupons is one of the most used for the calculation of the corrosion rate. Furthermore, a number of electrochemical methods for corrosion measuring exist and potentiodynamic polarization techniques are among the most popular. SEM-EDS is one of the main techniques used for examining and analyzing elemental surface component of corrosion-related samples [3]. The SEM examination provides information about the steel surface, specifically with regard to the morphology and corrosion type, while EDS is used for elemental analysis. Deposits on the surface can be amorphous or crystalline and XRD is used for identifying crystalline compounds.

It has been found that monitoring metal concentration (Fe, Cr and Ni) with ICP-MS during thermal degradation experiments gives essential information on the solvent corrosivity as presented in Grimstvedt et al. [4]. In that work, the iron concentration in the solvent from thermal degradation experiments was correlated with observed corrosion from pilot plant studies. Solvents with large iron concentrations after thermal degradation experiments showed high corrosion in the pilot plant. ICP-MS was a supplementary analytical instrument that was used for determining the solvent metal content of elements at pilot plants [4, 5].

Srinivasan et al. [6] studied the inhibition performance of a low toxic corrosion inhibitor in 30wt% MEA based solutions at 80 °C. They used cyclic potentiodynamic polarization and electrochemical impedance spectroscopy. In addition, they did surface analysis of carbon steel specimens by SEM and corrosion products were identified by XRD. From SEM, they observed distinct types of corrosion products. Xiang et al. [7] evaluated the electrochemical behavior of carbon steel at 30wt% MEA solutions with addition of Heat Stable Salts (HSS). At the initial stage, HSS increased the corrosion rate. They also mentioned that the presence of HSS can alter the inhibiting ability of the protective film.

The objective of this study is to evaluate and compare three analytical methods as potential tools for corrosion evaluation in MEA based CO<sub>2</sub> capture plants. For this purpose, analytical instruments i.e. ICP-MS, SEM-EDS and XRD are used for corrosion monitoring and characterization. We used ICP-MS to examine the relative corrosivity among different solutions. We used SEM-EDS to investigate if addition of a degradation product can affect the surface morphology and thus, if some specific degradation products has a catalytic role in corrosion. XRD was used for the identification of corrosion products. In addition, emphasis is given to which degradation products found in 30wt% MEA lead to corrosion and specifically to what extend they aggravate corrosion.

## Nomenclature

MEA	Monoethanolamine
HSS	Heat Stable Salts
HeGly	N-(2-hydroxyethyl) glycine
Bicine	N,N-Bis(2-hydroxyethyl) glycine
SEM	Scanning Electron Microscopy
EDS	Energy Dispersive X-ray Spectroscopy
ICP-MS	Inductively Coupled Plasma Mass Spectrometry
LC-MS	Liquid Chromatography Mass Spectrometry
XRD	X-ray Powder Diffraction

## 2. Materials and Methods

Two known degradation products of MEA, i.e. HeGly and Bicine, were tested for their corrosivity by placing CO<sub>2</sub> loaded 30wt% MEA solutions with 1wt% of degradation product in previously unused 316 SS cylinders at 135 °C for 5 weeks. Additionally 30wt% MEA without any addition of degradation compounds was tested. The solutions loading was 0.4 mol CO<sub>2</sub>/mol MEA. Details of the thermal degradation methodology are described by Fytianos et al. [8]. After the experiments, the solutions were analyzed for total metal concentration by ICP-MS. Higher metal concentrations in the solution correlates directly with higher corrosivity as discussed above [4]. Effects of corrosion on surface morphology and chemical composition of cylinders were examined by combined use of scanning electron microscopy (SEM) and energy dispersive spectrometry (EDS). Furthermore, the inner part of the cylinder was analysed with XRD for identification of corrosion products. Additionally, LC-MS was used for the quantitative analysis of MEA.

A high resolution Thermo Fischer Element 2 (Bremen, Germany) ICP-MS was used for the analysis of metals in the liquid samples. The solutions were analyzed for Fe, Cr, and Ni by ICP-MS as an indication of corrosivity. For the ICP-MS analysis each sample was mixed at room temperature and 100 µL was pipetted into a sample tube. 100 µL of concentrated HNO<sub>3</sub> (ultra pure) are added and everything was diluted to 10 mL with water. Finally this solution was further diluted resulting in a total dilution of 10000 (1 +9999).

Both SEM and EDS characterization were carried out by using a Hitachi S-3400N scanning electron microscope. For this purpose small pieces were cut from the cylinders and their surfaces were cleaned with ethanol to remove any deposited corrosion product prior to scanning. An acceleration voltage of 20.0 kV and a working distance of 10.0 µm were used, and samples were placed on stubs and scanned without coating. Aztec Energy software was used to process the EDS data.

Qualitative characterization of deposited corrosion products was conducted via powder X-Ray Diffraction (XRD) (D8 Advance DaVinci, Bruker AXS GmbH). The pattern was collected in the 2θ range of 20-80° using a Cu X-ray tube, with a step size of 0.013° and a step time of 0.78 s. Precipitates formed on cylinder walls were collected gently after air-drying, and crushed with a mortar and pestle before XRD analyses. The PDF-4+ database (from the International Centre for Diffraction Data) was used for species identification.

## 3. Results and Discussion

### 3.1. Liquid analyses

In Fig. 1 the MEA concentration after five weeks for the three solutions (30wt% MEA, 30wt% MEA+ 1wt% HeGly and 30wt% MEA+ 1wt% bicine) is shown. The original (week 0) amine concentration was 4.9 mol/kg (30wt% MEA). It can be seen that after 5 weeks, the loss of MEA is higher when HeGly or Bicine are added. After 5 weeks, the concentration of the loaded 30wt% MEA solution is 2.6 mol/kg. This result is almost the same with the MEA concentration after 5 weeks in a similar thermal degradation experiment of 30wt% loaded MEA (0.4 mol CO<sub>2</sub>/mol MEA) conducted by Vevelestad et al. [9]. In the cases of MEA+HeGly and MEA+Bicine, MEA concentration is 2.4 mol/kg. The difference in the MEA concentration between the 30wt% MEA solution and the 30wt% MEA+1wt% degradation product solutions is not big.

ICP-MS results for total Fe, Ni and Cr after five weeks are presented in Fig. 2. Higher metal concentration indicates more corrosion. The MEA+bicine solution had the highest Fe and Cr concentrations among the 3 solutions. MEA+HeGly had more Fe and Cr than MEA and the highest Ni concentration. There is coupling between solvent degradation and corrosion. Results from Fig. 2 show higher corrosion for MEA+Bicine followed by the MEA+HeGly solution. Moreover, the higher MEA loss (and therefore degradation) of MEA+HeGly and MEA+Bicine solutions compared with the 30wt% MEA solution of Fig. 1 can be compared to Fig. 2 giving an indication that with greater degradation, more corrosion will occur.

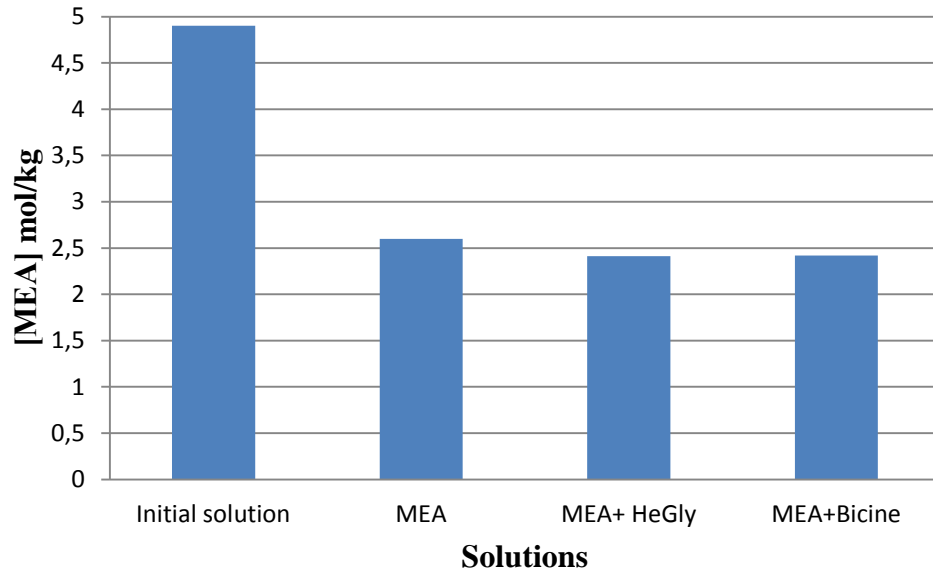


Fig. 1. MEA concentration after 5 weeks for different solutions containing 30wt% MEA + 1wt% degradation product. The first column on the left side is the initial concentration of the solutions before the experiment

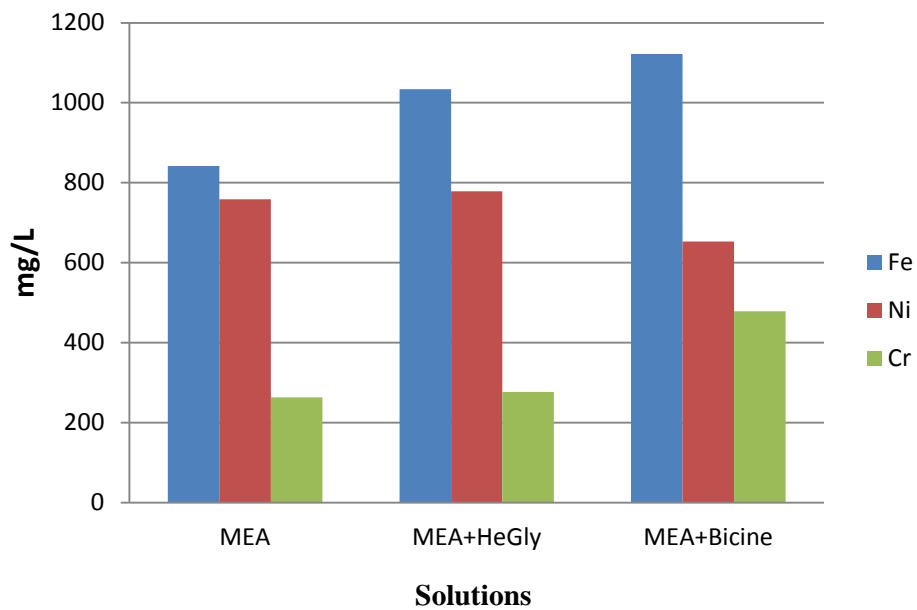


Fig. 2. ICP-MS results for total Fe, Cr, and Ni.

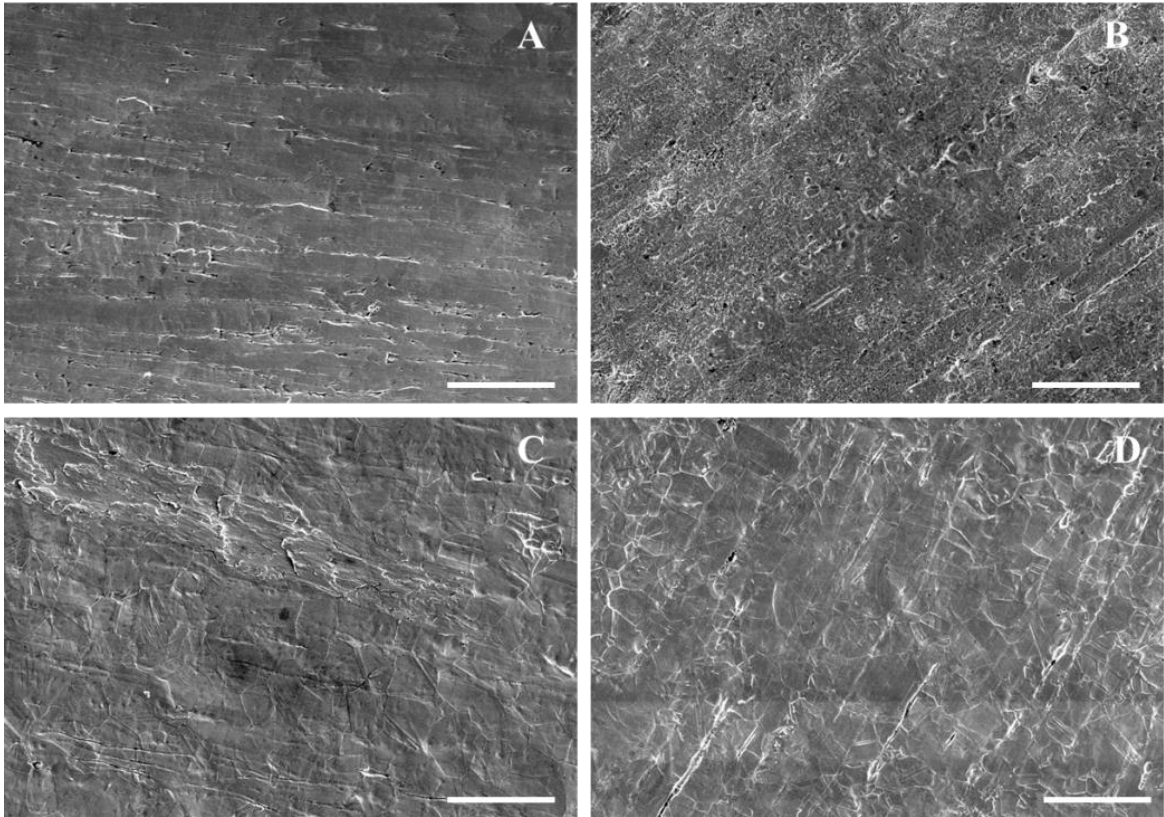


Fig. 3. SEM images of 316 stainless steel tube surface (A) before the experiment, (B) after 5 weeks for 30 wt% MEA solution, (C) 30 wt% MEA with 1 wt% bicine, (D) 30 wt% MEA with 1 wt% HeGly. Scale bars denote 100  $\mu\text{m}$ .

### 3.2. Cylinder surface analyses

Cylinder surfaces were examined by SEM and EDS at the end of the experiment in order to evaluate the effects of different solutions on corrosion from the surface morphology. The 30wt% loaded MEA solution without additional degradation product resulted in formation of a highly rough surface (Fig. 3B). On the other hand, in the presence of 1 wt% Bicine or HeGly in 30wt% MEA solution, crack formation was most prominent on the cylinder surfaces (Fig. 3C and Fig 3D). Differences in final surface morphology induced by corrosion can be evaluated as indicatives of varying corrosion mechanisms. Cylinder surfaces were confirmed to retain homogeneity after corrosion by elemental mapping via EDS (Fig. 4). Quantitative results of the surface compositions are given in Table 1. From Table 1, it can be observed that the elemental composition is similar for the various surfaces. The meaning of this will be discussed further in chapter 3.4.

Table 1. Elemental composition of 316 SS surfaces at the end of experiment for the corresponding solutions

wt %	MEA	MEA+Bicine	MEA+ HeGly
<b>Fe</b>	64.6	63.8	64.4
<b>Cr</b>	18.3	18.0	18.2
<b>Ni</b>	12.5	13.1	12.8
<b>Mo</b>	2.4	2.6	2.5
<b>Mn</b>	1.6	1.6	1.6

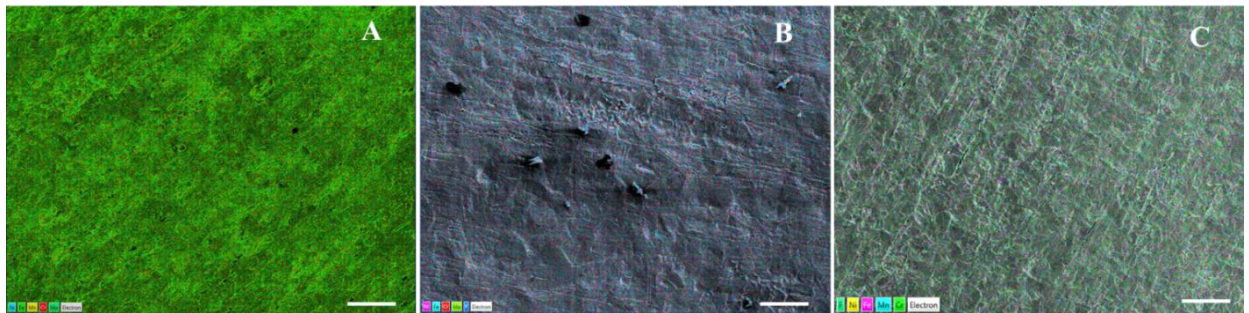


Fig. 4. EDS mapping of cylinder surfaces after 5 weeks at stripper conditions for (A) 30 wt% MEA solution, (B) 30 wt% MEA with 1 wt% bicine, and (C) 30 wt% MEA with 1 wt% HeGly. Scale bars denote 100  $\mu\text{m}$ .

### 3.3. Analyses of corrosion products on the surfaces

Corrosion products deposited on the surface of the 316 SS tubes were collected and qualitative analyses were conducted. XRD data showed formation of highly crystalline siderite,  $\text{FeCO}_3$ , on the cylinder surfaces for all the solutions. The role of iron carbonate in  $\text{CO}_2$  corrosion has been examined [10] and it was found that in the case of mild steel,  $\text{FeCO}_3$  forms a protective layer and decreases the corrosion rate. It was stated that protective film formation reduces the corrosion rate by blocking the metal surface rather than reducing the diffusion of corrosive species. Since  $\text{FeCO}_3$  was identified in all the tested 316 SS samples, further research on the effect of siderite on post-combustion  $\text{CO}_2$  capture is needed. A thin protective  $\text{FeCO}_3$  layer on carbon steel surfaces was also identified by Xiang et al. [7]. Additional low intensity peaks at  $43.5^\circ 2\theta$  associated with elemental iron, Fe, were observed in the MEA+1 wt% degradation product solutions. On carbon steel 1018,  $\text{Fe}_3\text{O}_4$  was the primary component of the surface layer along with the presence of elemental iron in the work of Srinivasan et al. [6].  $\text{Fe}_3\text{O}_4$  was not identified by XRD in the current work.

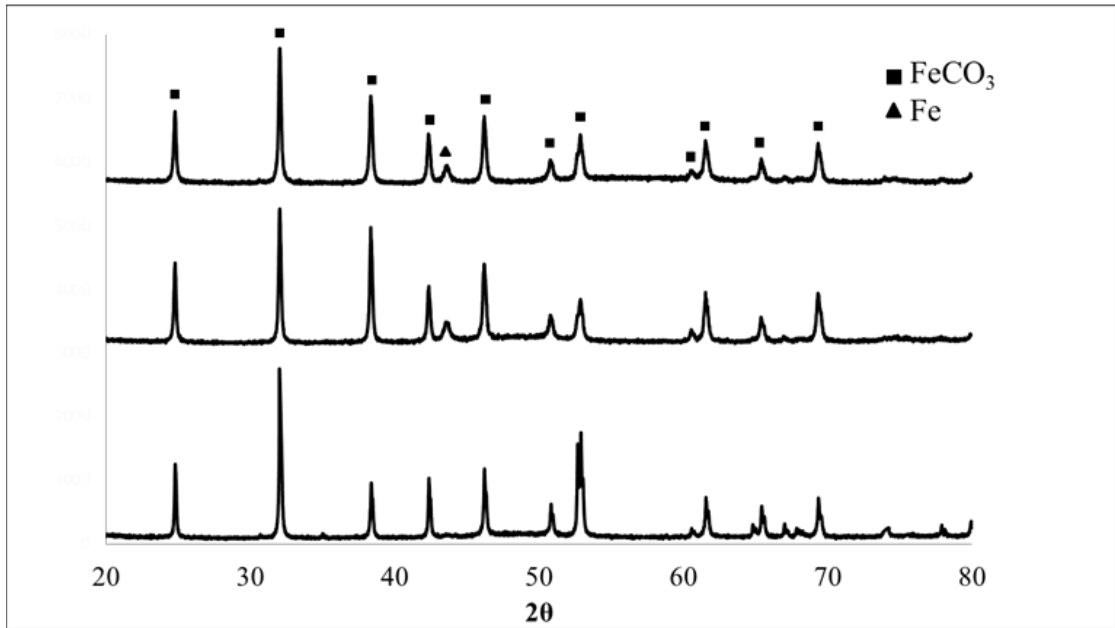


Fig. 5. XRD spectra of corrosion products collected from the cylinders of the 30 wt% MEA solution, 30 wt% MEA with 1 wt% bicine, and 30 wt% MEA with 1 wt% HeGly from bottom to top, respectively. Square dots denote peaks associated with  $\text{FeCO}_3$  and triangle dots denote crystalline Fe.

### 3.4. Discussion of the different methods

Liquid sample analysis with ICP-MS can work as a first screening of relative corrosivity among solutions but ICP-MS alone is not enough to study corrosion in post-combustion  $\text{CO}_2$  capture. ICP-MS does not give any details regarding corrosion type on the steel surface. Corrosion of the inner part of the stainless steel surface was characterized by using two analytical techniques (SEM-EDS and XRD) in order to provide a better understanding of the 316 SS surface corrosion type and corrosion products formation.

SEM itself can be used for surface morphology but does not give any details about the composition of the surface. EDS does not provide data about possible compounds that are formed on the surface but does give elemental composition. Different elemental composition for the various samples could indicate other corrosion products. In our work, the fact that  $\text{FeCO}_3$  was found in all of the samples together with EDS results which showed similar elemental mapping proved that no other major corrosion product was formed. By using only EDS without XRD, the accuracy in identifying possible compounds is limited. XRD is still the most accurate analytical technique for the identification of compounds on the steel surface.

Overall the results from SEM support the findings from the liquid analyses since ICP-MS showed higher relative corrosivity with the addition of HeGly and bicine. This was based on the fact that stainless steel surfaces had more cracks with the addition of degradation products. However, it is still difficult to correlate the ICP-MS findings with SEM results.

## 4. Conclusions

Corrosion evaluation of MEA solutions with three analytical instruments was performed. Total metal analysis with ICP-MS is a useful technique for the evaluation of corrosion because metal concentration in the liquid solution is correlated with corrosion. With SEM, the surface morphology and thus the corrosion type can be examined. EDS is used for the elemental composition of the surface and together with SEM, differences in the morphology can be examined in more detail. The corrosion product siderite,  $\text{FeCO}_3$ , was identified with XRD. Finally, it was concluded that the combination of the various techniques, gives a deeper understanding for the corrosion of stainless steel. The addition of a degradation product, in this case bicine and HeGly, was shown to increase the corrosivity of the  $\text{CO}_2$  loaded MEA 30wt% solution.

## Acknowledgements

The work is done under the SOLVIt SP4 project, performed under the strategic Norwegian research program CLIMIT. The authors acknowledge the partners in SOLVIt, Aker Solutions, Gassnova, EnBW and the Research Council of Norway for their support.

## References

- [1] Kohl, A., Nielsen, R. Gas Purification. Gulf Publishing Company, 1997.
- [2] J. Kittel and S.Gonzalez. Corrosion in  $\text{CO}_2$  post combustion capture with alkanolamines-A review. Oil & Gas Science and Technology- Rev. IFP Energies nouvelles, 2013, France.
- [3] Little B.J., Lee, J.S. Microbiologically Influenced Corrosion, John Wiley & Sons, Inc., Hoboken, New Jersey, 2007, pp. 28-34.
- [4] Andreas Grimstvedt, Eirik Falck da Silva and Karl Anders Hoff. Thermal degradation of MEA, effect of temperature and  $\text{CO}_2$  loading. TCCS7, SINTEF Materials and Chemistry, 7465 Trondheim.
- [5] Purvil Khakharia, Jan Mertens, Arjen Huizinga, Séverine De Vroey, Eva Sanchez Fernandez, Sridhar Srinivasan, Thijs J.H. Vlugt, and Earl Goetheer. Online Corrosion Monitoring in a Postcombustion  $\text{CO}_2$  Capture Pilot Plant and its Relation to Solvent Degradation and Ammonia Emissions. Ind. Eng. Chem. Res., 2015, 54 (19), pp 5336–5344.
- [6] Sureshkumar Srinivasan, Amornvadee Veawab, Adisorn Aroonwilas. Low Toxic Corrosion Inhibitors for Amine-based  $\text{CO}_2$ . Energy Procedia. Volume 37, 2013, Pages 890-895
- [7] Yong Xiang, Maocheng Yan, Yoon-Seok Choi, David Young, Srdjan Nesic. Time-dependent electrochemical behavior of carbon steel in MEA-based  $\text{CO}_2$  capture process. International Journal of Greenhouse Gas Control 30 (2014) 125–132.
- [8] Fytianos G., Grimstvedt A., Knuutila H., Hallvard F. S. Effect of MEA's Degradation Products on Corrosion at  $\text{CO}_2$  Capture Plants. Energy Procedia, Volume 63, 2014, Pages 1869-1875.
- [9] Vevelstad S.J., Grimstvedt A., Knuutila H. and Svendsen H.F., “Thermal degradation on already oxidatively degraded solutions.”, Energy Procedia, 37(2013), 2109-2117.
- [10] Nešić S, Lee K-LJ. A mechanistic model for carbon dioxide corrosion of mild steel in the presence of protective iron carbonate films—part 3: film growth model. Corrosion 2003; 59:616–28